



This is a repository copy of *Comparison of the burning of a single diesel droplet with volume and surface contamination of soot particles.*

White Rose Research Online URL for this paper:
<https://eprints.whiterose.ac.uk/169388/>

Version: Accepted Version

Article:

Abdul Rasid, A.F. and Zhang, Y. orcid.org/0000-0002-9736-5043 (2021) Comparison of the burning of a single diesel droplet with volume and surface contamination of soot particles. *Proceedings of the Combustion Institute*, 38 (2). pp. 3159-3166. ISSN 1540-7489

<https://doi.org/10.1016/j.proci.2020.07.092>

Article available under the terms of the CC-BY-NC-ND licence
(<https://creativecommons.org/licenses/by-nc-nd/4.0/>).

Reuse

This article is distributed under the terms of the Creative Commons Attribution-NonCommercial-NoDerivs (CC BY-NC-ND) licence. This licence only allows you to download this work and share it with others as long as you credit the authors, but you can't change the article in any way or use it commercially. More information and the full terms of the licence here: <https://creativecommons.org/licenses/>

Takedown

If you consider content in White Rose Research Online to be in breach of UK law, please notify us by emailing eprints@whiterose.ac.uk including the URL of the record and the reason for the withdrawal request.



eprints@whiterose.ac.uk
<https://eprints.whiterose.ac.uk/>

Comparison of the Burning of a Single Diesel Droplet with Volume and Surface Contamination of Soot Particles

Ahmad Fuad Abdul Rasid^{1,a,*} and Yang Zhang^{2,b}

¹a.fuad@utem.edu.my, +6(0)178407548,

²yz100@sheffield.ac.uk, +44(0)1142227880

^a *Fakulti Teknologi Kejuruteraan Mekanikal dan Pembuatan (FTKMP), Kampus Teknologi, Universiti Teknikal Malaysia Melaka, Hang Tuah Jaya, 76100 Durian Tunggal, Melaka, Malaysia.*

^b *Department of Mechanical Engineering, The University of Sheffield, Sir Frederick Mappin Building, Sheffield, S1 3JD, United Kingdom*

Colloquium

Spray, Droplet, and Supercritical Combustion – Combustion of droplets

Total length of paper

Figure	Word Count (Method 1)	Sections	Word Count
1	203	Introduction	585
2	114.8	Experimental Setup	681
3	627.44	Results and Discussions	2143
4	219.12	Conclusions	423
5	142.52	Figures	1939.12
6	321	Equations	N/A
7	146.36	References	402.04
8	165	Acknowledgement	26
Total	1939.12	Total words	6199.16

List of Figures

- Fig. 1 Experimental setup
- Fig. 2 Combustion phases of diesel droplet
- Fig. 3 Repetitive measurement on D^2 regression of (a) neat, (b) SC, (c) 0.1% VC, (d) 0.2% VC, (e) 0.3% VC and (f) 0.4% VC diesel droplets
- Fig. 4 Average of instantaneous burning rate constant between (a) neat and 0.2% VC diesel and (b) SC and 0.4% VC diesel.
- Fig. 5 Liquid-phase visualisation on VC droplet
- Fig. 6 Burning rates and combustion phases of neat, SC and VC droplets
- Fig. 7 Disruptive burning of VC droplet with particle mass loading of (A) 0.2% and (B) 0.3%
- Fig. 8 Flame stand-off ratio of neat, SC and VC droplets

Abstract

Following an examination on the effect of soot contamination on the surface of a diesel droplet to the combustion characteristics, an investigation on a uniform suspension of diesel soot particles within a diesel droplet was conducted experimentally for the first time. The aim is to determine the effect of uniformly suspended soot to the evaporation characteristics of a diesel droplet. Soot formed by the combustion of diesel was collected and suspended uniformly within a neat diesel. The particle loadings were varied from 0.1% to 0.5% by mass and ignited in a single isolated droplet, normal gravity and ambient condition. It is found that the burning rate of contaminated droplets is lower than the neat condition in all particle loading. A critical loading was identified to be at 0.2% which has shown a slight improvement of the burning rate despite having a reduced rate compared to its neat counterpart. It is found that within the critical loading, the particle briefly improves the thermal conductivity towards the core of the droplet which in turn slightly enhances the evaporation rate. Once the shear stress exerted by the external gas flow is subjected to the droplet, the internal circulation is induced and moves the particle towards the surface of the droplet. Agglomeration of particles on the surface of the droplet inhibit the liquid diffusion from the core to the surface of the droplet thus suppressing the evaporation rate. High particle loading would accelerate the agglomeration process whereas a low and critical particle loading briefly improves the evaporation in a reduced condition. These insights are of significance for determining the main cause of the detrimental effect from soot contamination in a liquid fuel; providing a base approach upon identifying the role of nanoparticles within the fuel droplet combustion study.

Keywords: Droplet combustion; Soot contamination; Liquid-phase visualisation; Disruptive burning; Combustion Lifetime

1.0 Introduction

Nanofluids is a colloidal suspension of either metallic or non-metallic particles [1]. During the steady combustion phase, some distortion on the droplet surface is observed. Particles inside the bubble heat up the droplet locally, initiating a heterogeneous nucleation. The steady stage ended when the bubble ruptured the droplet with a strong puff [2]. In addition, three distinguish phases were observed involving steady combustion, shell formation and microexplosion [3] which in turn deviates the surface regression from the D^2 -law [2, 4]. The particles have the tendency to accumulate on the droplet surface [5] which initiates multiple nucleation sites of vapour bubbles. Weak microexplosion occurs towards the end of the steady regression and becomes more aggressive towards the end of the droplet lifetime due to a higher concentration of agglomerated particles. It is also reported by Ghamari & Ratner [6] that some particles are observed to be ejected from the droplet surface and burned with a glowing char.

On the other hand, soot is a nano-sized particle with a size ranging from 10 to 50 nm [7, 8]. During a continuous combustion process in a compression ignition engine, there is a possibility of soot to contaminate the fuel droplet contained in the spray [9, 10]. Rasid & Zhang [3] conducted an experiment to determine the mechanism of soot contamination on diesel fuel droplet. They observed that the soot contained in the hot combustion gas is immediately quenched on the surface of the droplet on contact and forms a shell of agglomerated particles. This formation suppressed the evaporation rate and reduces the combustion stability. It was concluded that the early formation of the shell on the surface of the droplet reduces the liquid mass diffusion from the core towards the surface. The suppression of the evaporation rate is also observed during the combustion of nanofluid droplet with excessive particle mass loading [4, 6] due to the formation of the agglomerated shell on the surface of the droplet.

These observations suggest that the formation of the shell on the surface would be detrimental to the combustion characteristics and the effect is more profound in the work conducted by Rasid & Zhang [3] who demonstrated early formation of a soot shell on the surface of the droplet during a contamination process. On the other hand, a uniform suspension of nanoparticles within the base fuel would improve the combustion characteristics under certain critical mass loading due to the enhanced thermal radiative absorption and the

effect of thermal bridging provided by the scattered particles within the droplet [11]. Hence, it is highly suggested that a uniform distribution of nanoparticles within the droplet would enhance the combustion characteristics of a base fuel. Under these reasons, this paper investigates the combustion behaviour of a diesel droplet suspended with a uniform distribution of soot particles. The aim is to identify the combustion characteristics and particle dynamics of a diesel droplet with uniform suspension of soot particles termed as volume-contaminated (VC) diesel droplet in this paper and comparing them with the surface-contaminated (SC) diesel droplet previously conducted by Rasid & Zhang [3]. A Homogeneous distribution of soot tested in the present work is to determine the evaporation behaviour of VC and compare it with SC diesel droplet conducted in the previous paper. The application of these findings focuses on the fundamental understanding of shell formation during the evaporation of droplet with particle loadings. Furthermore, detailed quantitative measurements were done to identify the particle condition which would enhance or diminish a nanofluid combustion properties.

2.0 Experimental Setup

A commercial diesel fuel was used in this experiment; with the exact same properties of the fuel used in the previous work of Rasid & Zhang [3] to ensure meaningful comparative results between a neat, surface contaminated and volume contaminated diesel droplet combustion. A Phantom V210 high speed camera was used to image the droplet evolution via a backlighting setup shown in Fig. 1. A Nikon Micro NIKKOR 60mm f/2.8D with an extension tube was mounted on the camera for high magnification of droplet visualisation (x40) during the capturing speed of 10000 fps. Simultaneous visualisation of flame formation was done by placing a Photron-SA4 high speed colour camera perpendicular to the backlit setup with a Nikon AF Nikkor 50 mm f/1.8D lens. Direct visualisations of the flame were done with a magnification of x5 and recording speed of 500 fps. The initial diameter of all fuel sample suspended on a 100 μm silicon carbide fibre was ensured to be 1 ± 0.05 mm before ignition. The droplet was ignited by placing a heating wire, made up of Kanthal 1 mm below the droplet. The wire was heated up to 800 °C before insertion and removed upon the first appearance of a flame.

Specific algorithms were constructed using Matlab image processing tools which were able to identify the droplet boundary and recorded the instantaneous size of the imaged droplets throughout their lifetime.

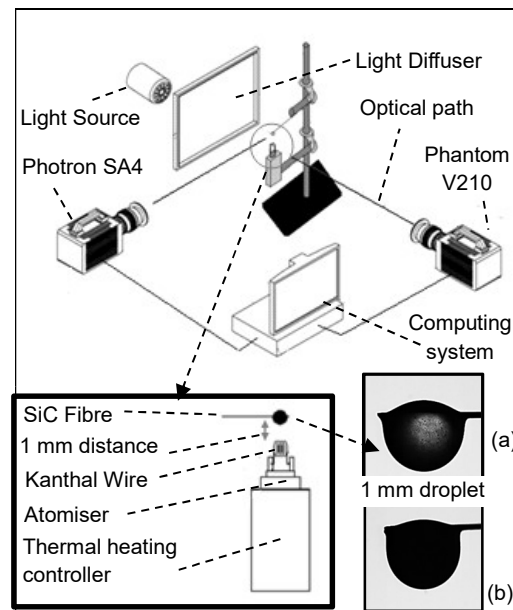


Fig. 1 Experimental setup

2.1 Sample Preparations

The diesel soot was collected from particle deposition on a flat glass during the burning of diesel fuel through a fibre glass-reinforced wick. The deposited particles are then scrapped by a spatula into a glass bottle and weighted. VC diesel droplet were prepared by adding the particles into a diesel fuel with 0.1% to 0.5% particle loadings by mass. It is stated from various studies on carbon-based nanofluid droplet combustion [6, 12, 13] that the critical mass loading of nanoparticle for enhanced combustion characteristics are between 0.1 to 0.5%. Under these reasons, those particular mass loading of soot particles were investigated since the diesel soot is made up of mostly carbon-based particles. No surfactant was added to prevent significant change to the fuel properties of the base fuel [1]. The droplet is transparent up until 0.1% mass loading as shown in Fig. 1(a) and turned opaque when the particle mass loading increased to 0.2% as shown in Fig 1(b).

2.2 Combustion Phases

Discussions on combustion phases in this paper are referring to the diagram shown in Fig. 2; taken from one regression of the droplet squared diameter of a burning diesel droplet. Upon ignition, the droplet begins to swell and expand due to thermal expansion, denoted as Phase I. The main characteristics of this phase is shown by the non-linear curve in the regression of D^2 which indicates the continuous process of both expansion and evaporation [14]. Hence, the measurement of the droplet evaporation and burning rate does not account for the regression during this phase.

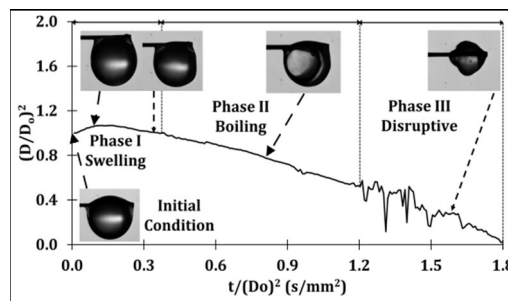


Fig. 2 Combustion phases of diesel droplet

As soon as the droplet heating effect diminishes, the regression of D^2 is shown to linearly reduce. According to Law and Sirignano [15], high evaporation rate of a fairly large droplet (1 mm) would have a temperature gradient along the surface to the core of the droplet that varies with time. During this phase, D^2 reduces linearly with time and conforms with the D^2 -law [16]. Hence, this phase is denoted as Phase II (boiling) and the measurement of the evaporation and burning rate were made within the period of this phase.

Over time, the surface regressed disruptively as the droplet surface becomes more viscous resulting from fuel decomposition [17]. Also, some particle is observed to be trapped inside the droplet which in turn initiates a heterogeneous nucleation of a vapour bubble within the droplet. Upon surface rupture, the liquid from the bottom of the bubble periphery pushed the liquid outwards and ejects multiple sub-droplets. The sudden loss of liquid mass deviated from the D^2 regression of the D^2 -law and the measurement of the evaporation rate during this phase is unreliable [6]. This phase is denoted as Phase III (disruptive).

3.0 Results and Discussions

Measurements of the evolution of droplet diameter were made on VC diesel droplets with up to 0.5% soot particle mass loading and is presented in Fig. 3. Measurement of D^2 shows good repeatability in each sample thus making the analyses done in the present work to be considered reliable. In low mass loading of 0.1%, the regression is steady with minor puffing recorded throughout the lifetime of the droplet. When the loading increased to 0.2%, the regression of D^2 fluctuates rapidly in Phase II with the highest magnitude of distortion. This is believed to have occurred due to a multiple heterogeneous nucleation of a vapour bubble that emerged within the droplet [18]. As a result, more puffing process occurred [19]. However, when the loading increased to 0.3%, the frequency and magnitude of the fluctuation on D^2 regression began to reduce and it was observed to be steadier when the loading was further increased.

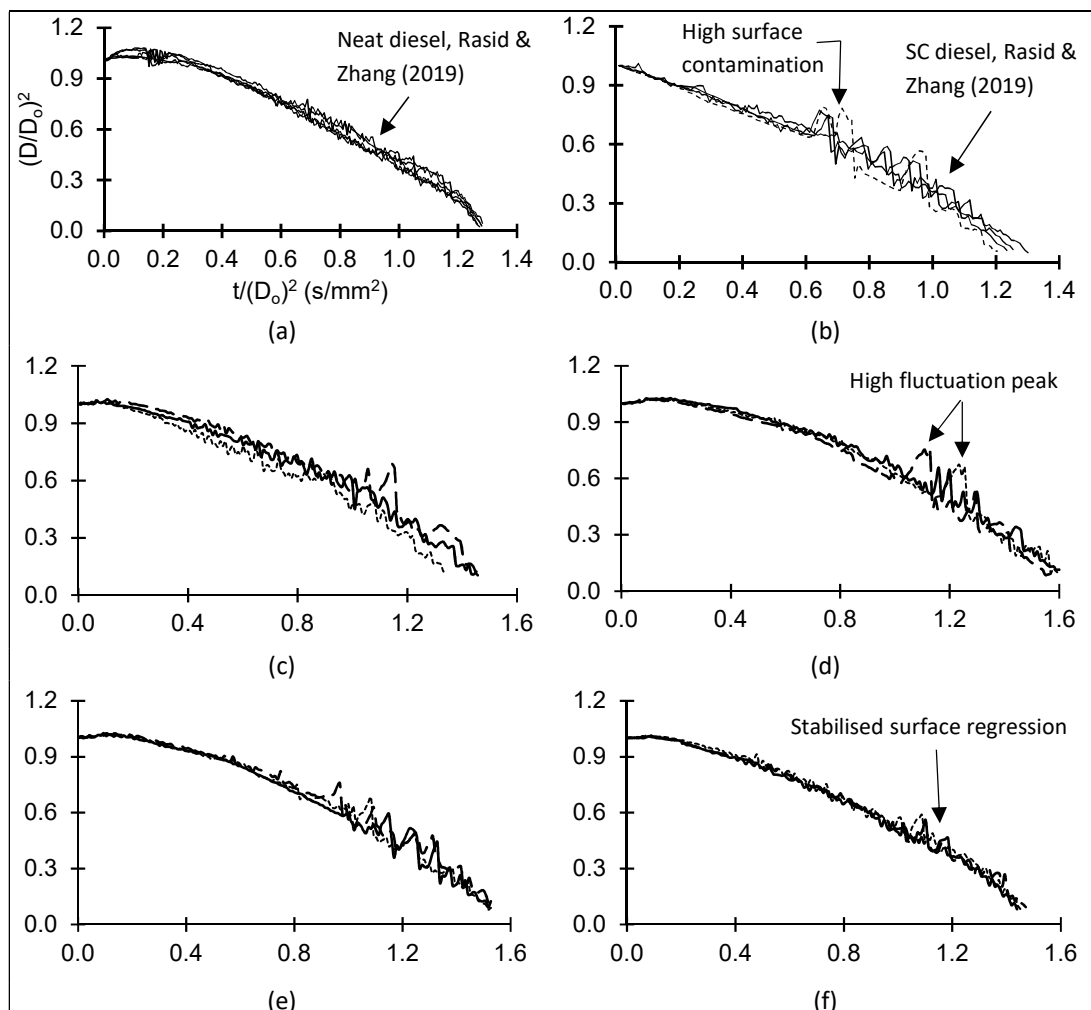


Fig. 3 Repetitive measurement on D^2 regression of (a) neat, (b) SC, (c) 0.1% VC, (d) 0.2% VC, (e) 0.3% VC and (f) 0.4% VC diesel droplets

On the other hand, the period of droplet heating has shown to be increased by a longer curve of the D^2 regression during the early droplet lifetime as the particle loading increases indicating a higher amount of heat from the combustion being absorbed [12] by the soot particles rather than being used to heat the liquid fuel. Comparing the surface instabilities of burning VC to the SC droplet analysed by Rasid & Zhang [3], it is found that higher particle loading in VC droplet stabilises the droplet surface regression whereas higher contamination of particles in SC droplet increases the surface instabilities. Such differences indicate that the dynamics of the suspended particle plays an important role on the evaporation behaviour of contaminated droplet.

Fig.4 shows the average measurement of an instantaneous burning rate constant of neat, SC diesel, 0.2% VC diesel and 0.4% VC diesel. Neat diesel comprises several combinations of volatile mixtures, which are expected to evaporate disruptively due to their differences in component's volatility. Regression of 0.2% VC diesel as shown in Fig. 4(a) spikes towards the end of its lifetime, similar to the neat diesel droplet. It is found that during the combustion instabilities of both droplets, strong puffing occurs which in turn ejecting some liquid outwards, contributing to a higher mass loss during the combustion processes [3]. On the other hand, the SC diesel and 0.4% VC diesel shows weak puffing occurs throughout the combustion. It is known that a low puffing strength would only releases vapour trapped inside the droplet without any significant loss of liquid mass. Strong puffing during the combustion of neat and 0.2% VC diesel is expected to elevate the burning rate of both fuels.

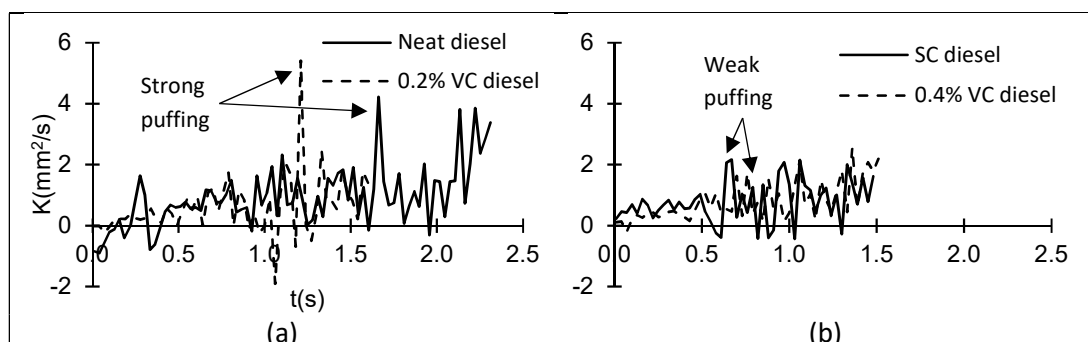


Fig. 4 Average of instantaneous burning rate constant between (a) neat and 0.2% VC diesel and (b) SC and 0.4% VC diesel.

3.1 Liquid-phase Visualisations

To further understand such changes in the combustion behaviour, the dynamics of the particle within the droplet were monitored. Fig. 5 shows sequential visualisation on a VC droplet with 0.05% particle mass loading. This loading was selected to be demonstrated here due to its transparent droplet appearance, making the observation on the particle dynamics inside the droplet possible. Upon ignition, the particles inside the droplet starts to move with the aid of internal circulation induced by buoyancy, known as orthokinetic aggregation [2]. Some of the particles began to agglomerate as shown at $t = 172.5$ ms. The segregated particles near the surface of the droplet is oxidised in the early lifetime of the droplet shown by the darker combustion gas at 513.5 ms.

As the combustion progressed, the soot particle is shown to have formed a shell on the surface of the droplet at $t = 797.1$ ms. It can be seen that the suspended soot was difficult to be oxidised once they had fully agglomerated. The tendency of soot to move towards the surface of the droplet is due to its composition which is made up of a mostly hydrophobic element [20], that would move to an area with less liquid being subjected to its surface area. As the droplet continues to evaporate and shrinks in size at $t = 1049.9$ ms, the shell is shown to have fully enveloped the droplet which forms a barrier that would obstruct any escaping fuel vapour through the surface.

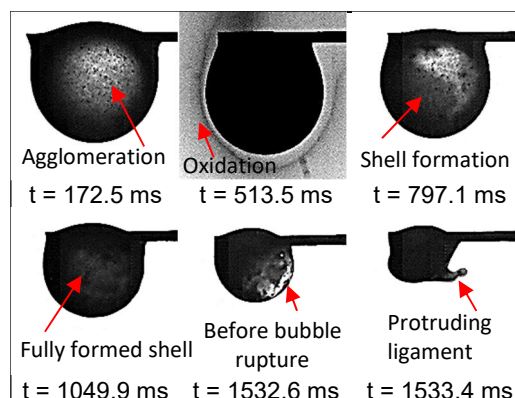


Fig. 5 Liquid-phase visualisation on VC droplet

The nucleated bubble formed due to a heterogeneous nucleation inside the droplet expands and moved towards the surface with the thinnest shell before the surface ruptured. This is shown by the more

transparent area on the surface of the droplet at $t = 1532.6$ ms. Once the surface of the droplet ruptured during bubble breakup, a ligament of liquid fuel protruded outward which ejected a sub-droplet outward. The dynamic of particles within the VC droplet are shown by sequential images in Fig. 5. It is found that the particle dynamics within the droplet are similar in each particle loading. However, the dynamics of soot particles inside the droplet with 0.2% particle loading and beyond cannot be observed due to their opaque appearances. Nevertheless, the occurrences of puffing and sub-droplet ejection were observed in each sample and are identified by the fluctuation in the regression of D^2 in Fig. 3 and Fig. 4. Several similarities of particle dynamics are found between VC and SC droplet conducted in the previous work [3]. It is found that the soot particle has high tendency to reside on the surface of the droplet and immediately forms a shell as they agglomerated.

3.2 Burning rate and Combustion Phases

The burning rates of VC droplets were measured and compared with neat and SC droplet as shown in Fig. 6. A uniform suspension of soot particle is found to have significantly reduced the burning rate of neat diesel in all mass loading. The burning rate reduced sharply in low particle loading of 0.1%, began to slightly increase to a peak in 0.2% and continue to reduce when the loading is increased further. From the observation made on the liquid-phase dynamics, it is known that the soot contained inside the droplet undergoes a rapid agglomeration process. Due to the similar location of an agglomerated soot shell to the SC diesel droplet discussed by Rasid & Zhang [3], the reduction in burning rate of VC droplet is well understood. The shell inhibits the liquid diffusion from the core towards the surface of the droplet which in turn suppressed the evaporation rate [5].

The mass loading of soot is found to be critical around 0.2% with the highest burning rate among other loadings of VC droplets. As shown by the liquid-phase dynamics in Fig. 5, the VC droplet undergoes strong puffing and sub-droplet ejections during combustion. From the regression of D^2 shown in Fig. 3(d), the fluctuation is more severe during the combustion of the VC droplet with a 0.2% soot mass loading. This indicate the occurrences of more rapid puffing and sub-droplet ejections which in turn is making the 0.2% VC droplet to have higher mass loss of liquid fuel through a vapour nucleation process especially during PII. Higher particle

loading forms a sturdier shell of agglomerated soot, obstructing any fuel vapour from being ejected through the surface. In addition, more heat is absorbed by the thicker shell enveloping the droplet thus slowing the heating process towards the core of the droplet. As a result, the most evaporation only occurs near the formation of a shell with minimal internal bubble nucleation and the evaporation progresses with the least disruption.

The bar graph shown during Phase I indicates the increase in duration of the droplet heating process when the soot particle loading is increased. According to Kittelson [21], the absorbance of visible light by soot is high compared to the scattering due to the high carbon content of the particle. Hence, the soot tends to act as a heat sink which absorb most of the heat from the flame during the early combustion process. Once the temperature of the soot shell is sufficiently high, it acts as a heat source that starts to heat the liquid droplet toward its boiling point. This process delayed the onset of the liquid heating thus prolongs the duration of PI.

The steady burning phase of the VC droplet is shortened to a similar duration between each loading. It is shown that as long as there is soot contaminating the droplet, the duration of PII shortens regardless of any particle loading, similar to a SC droplet. In VC droplet combustion, the contamination only affected the duration of droplet heating (PI) and the disruptive phase (PIII) when the particle mass loading is varied. Longer duration of PIII is shown by the bar chart in Fig. 6 in low particle loading. This is caused by the occurrences of sub-droplet ejections of the VC droplet with mass loading up to 0.2%. The soot shell in 0.1% loading is thinner which allows more puffing of fuel vapour and sub-droplet ejection to occur thus transitioned from PII combustion to PIII earlier. With minimum mass loss of liquid fuel on VCD droplets that has soot mass loading higher than 0.2%, their duration of disruptive phase is equivalently low.

From the previous study of Rasid & Zhang [3] on SC droplets, it is found that the burning rate reduces when the soot particle is quenched on the surface of the droplet and remained constant between each contamination density. However, the degree of reduction varies between mass loading of VC droplets measured in the present work. Such a difference is attributed to the dynamics of soot particles contaminating the droplet. In the case of SC droplet, the soot forms a shell of agglomerated particles on the surface of the droplet prior to ignition. As a result, the liquid diffusion of the droplet is inhibited throughout the lifetime of the droplet resulting in similar reduction of burning rate regardless of surface contamination densities. On the

other hand, the agglomeration rate of particles in VC is highly depended on the initial particle mass loading. Higher loading promotes a faster agglomeration rate [2] which in turn forms earlier obstructive shell in PII resulting further reduction of the burning rate. The slower agglomeration of particles in critical loading of 0.2% provides sufficient time for the particle within the droplet to enhance the burning rate with enough particles acting as a thermal bridge [11] and initiates multiple heterogeneous nucleation sites within the droplet.

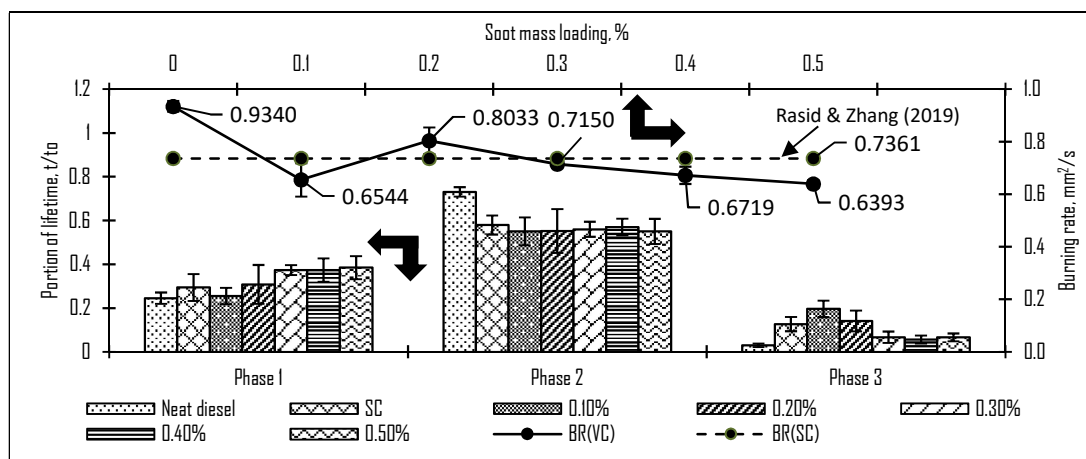


Fig. 6 Burning rates and combustion phases of neat, SC and VC droplets

3.3 Disruptive Evaporation

To further understand the differences in disruptive burning between low and high particle loadings, sequential images of liquid and particle ejections are presented in Fig. 7. For particle loading of 0.2% and below, a typical sub-droplet ejection process is shown in Fig. 7(A). The droplet combustion is unable to oxidise the soot particles once they have completely agglomerated thus turning the droplet opaque in appearance. The ejected sub-droplet of VC contains soot particles as indicated by the colour of the flame in the image at $t = 1355$ ms. The bright orange-coloured flame indicates the oxidation of soot contained inside the ejected sub-droplet. A similar ejection process occurred multiple times within the disruptive phase, further explaining the cause of liquid mass loss that prolongs the duration of PIII.

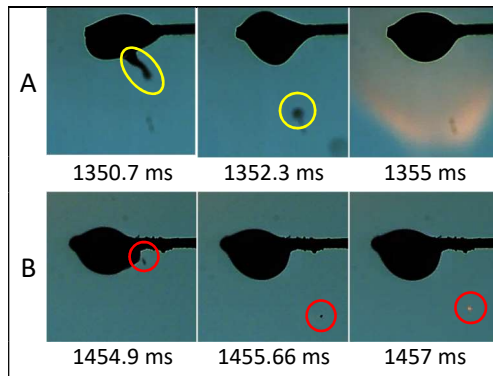


Fig. 7 Disruptive burning of VC droplet with particle mass loading of (A) 0.2% and (B) 0.3%

A typical disruptive burning process of a VC droplet with particle loading above the critical loading of 0.2% is shown in Fig. 7(B). During this phase, an agglomerated soot particle is observed to be ejected through the surface of the droplet. Although the puffing intensities are lower, the agglomerated particles on the surface of the droplet is more densely packed. Slight puffing during the combustion ejects a small amount of volatile vapour together with a chunk of agglomerated particles outward. The certainty of the ejected matter to be a soot particle is shown in the image at $t = 1457$ ms by the smouldering particle once it is transported to the flame region. The ejection of particle mildly distorts the surface of the droplet which explains the lower intensities of fluctuation recorded in the D^2 regression.

3.4 Flame Formation

Fig. 8 shows the comparison of flame stand-off ratio (FSR) between neat and VC diesel droplet with a mass loading from 0.1% to 0.5%. The reduced burning rate of VC droplet in all loadings lowered the FSR for the entire droplet lifetime. Some vapour accumulation effect is present as shown by the slight increase of FSR during PII. Similar to SC droplet combustion, the FSR is found to be declining towards the end of the droplet lifetime. A slight elevation of FSR during sub-droplet ejection is shown for a VC droplet with particle mass loading below the critical value of 0.2% indicating the gas-phase interaction between the flame of ejected sub-droplet and the parent droplet. Regressions of FSR for mass loading beyond the critical value are observed to have sharply declined due to non-interacting combustion between smouldering soot particle and the

enveloped flame of the parent droplet. With synchronised visualisation of droplet liquid-phase and flame formation conducted in the present work, the decline of burning rate and FSR is fully identified.

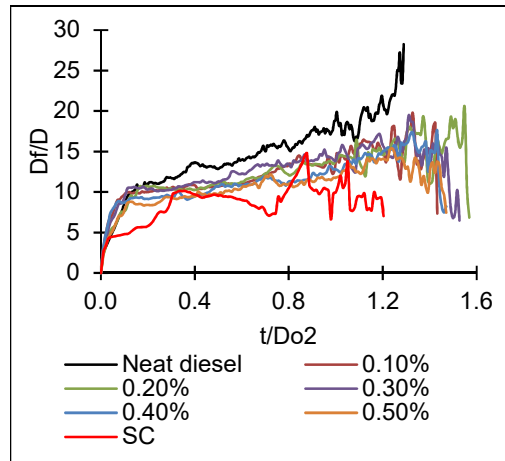


Fig. 8 Flame stand-off ratio of neat, SC and VC droplets

4.0 Conclusions

With sufficient quantitative measurements carried out on the combustion of soot contaminated diesel droplet conducted in this paper, the influences of soot particles resided inside and on the surface of the base fuel droplet are determined. Several conclusions are derived from the present work includes:

1. The critical loading of volume-contaminated (VC) droplet is found to be around 0.2%. The slight increase in burning rate is observed to be caused by the frequent puffing during the steady burning phase. This indicates a higher amount of liquid evaporation by means of bubble nucleation and liquid-gas diffusion on the surface of the droplet. The shell formed on the surface is thin enough to allow nucleated vapour bubble to escape through the surface. Higher particle loading retarded the heat transfer towards the core of the droplet. As a result, no vapour bubble nucleates within the droplet. Hence, the evaporation rate is reduced with only a liquid-gas diffusion process occurring on the surface of the droplet.
2. As long as there is a soot particle contaminating the fuel droplet, the burning rate is found to have significantly reduced. The differences of burning rate between SC and VC droplet is determined to be affected by their differences in the particle agglomeration rate. Soot particles on the SC droplet had

completely agglomerated into a shell prior to ignition which in turn significantly reduces the burning rate throughout the droplet lifetime. On the other hand, the soot contained within the VC droplet only began to agglomerate once the droplet reaches the end of Phase I; providing sufficient time for the particles within the droplet to briefly enhance the heat conduction in critical mass loading. Higher loading has a more rapid agglomeration rate which explains the declining burning rate. The delay of particles to be completely agglomerated into a shell varies the burning rate between each loading of a VC droplet. It is found that as soon as the soot particle completely agglomerated to a soot shell, the evaporation of the contaminated fuel droplet is suppressed.

3. The effect of fuel vapour accumulation reduces when the droplet is contaminated by soot particles due to the suppressed evaporation. This is evaluated by the decline of FSR towards the end of the droplet lifetime. In addition, the ejected matter during the disruptive burning phase contains mostly agglomerated soot particles. The burning and oxidation of the ejected mixture outside the droplet is observed to have no gas-phase interaction with the parent droplet resulting in the FSR to decline as the combustion progresses.

5.0 Acknowledgements

The authors would like to thank Universiti Teknikal Malaysia Melaka for the Fellowship Scheme and the Ministry of Higher Education Malaysia for SLAB Scholarship Scheme

6.0 References

- [1] A. K. Yadav, K. Nandakumar, A. Srivastava, and A. Chowdhury, Combustion of rocket-grade kerosene droplets loaded with graphene nanoplatelets—A search for reasons behind optimum mass loadings, *Combust. Flame*, 1 203 (2019) 1–13.
- [2] Y. Gan and L. Qiao, Combustion characteristics of fuel droplets with addition of nano and micron-sized aluminum particles, *Combust. Flame* 158 (2) (2011) 354–368.
- [3] A. F. A. Rasid and Y. Zhang, Combustion characteristics and liquid-phase visualisation of single isolated diesel droplet with surface contaminated by soot particles, *Proc. Combust. Inst* 37 (3) (2019) 3401–3408.
- [4] I. Javed, S. W. Baek, and K. Waheed, Autoignition and combustion characteristics of heptane droplets with the addition of aluminium nanoparticles at elevated temperatures, *Combust. Flame* 162 (2015) 191–206.

- [5] H. Li, C. D. Rosebrock, N. Riefler, T. Wriedt, and L. Mädler, Experimental investigation on microexplosion of single isolated burning droplets containing titanium tetraisopropoxide for nanoparticle production, *Proc. Combust. Inst* 36 (1) (2017) 1011–1018.
- [6] M. Ghamari and A. Ratner, Combustion characteristics of colloidal droplets of jet fuel and carbon based nanoparticles, *Fuel* 188 (2017) 182–189.
- [7] F. Tao, V. I. Golovitchev, and J. Chomiak, A phenomenological model for the prediction of soot formation in diesel spray combustion, *Combust. Flame* 136 (3) (2004) 270–282.
- [8] C. T. Avedisian, Recent Advances in Soot Formation from Spherical Droplet Flames at Atmospheric Pressure, *J. Propuls. Power* 16 (4) (2008) 628–635.
- [9] D. Kittelson and M. Kraft, Particle Formation and Models in Internal Combustion Engines, Reports no. 142, Cambridge Centre for Computational Chemical Engineering, 2014.
- [10] S. Mosbach *et al.*, Towards a detailed soot model for internal combustion engines, *Combust. Flame* 156 (6) (2009) 1156–1165.
- [11] S. P. Jang and S. U. S. Choi, Role of Brownian motion in the enhanced thermal conductivity of nanofluids, *Appl. Phys. Lett* 84 (2004) 4316.
- [12] S. Tanvir and L. Qiao, Droplet burning rate enhancement of ethanol with the addition of graphite nanoparticles: Influence of radiation absorption, *Combust. Flame* 166 (2016) 34–44.
- [13] Y. Gan and L. Qiao, Optical properties and radiation-enhanced evaporation of nanofluid fuels containing carbon-based nanostructures, *Energy Fuels* 26 (7) (2012) 4224–4230.
- [14] M. Zhu, Y. Ma, and D. Zhang, Effect of a homogeneous combustion catalyst on combustion characteristics of single droplets of diesel and biodiesel, *Proc. Combust. Inst* 34 (1) (2013) 1537–1544.
- [15] W. A. Sirignano and C. K. Law, Unsteady Droplet Combustion and Droplet Heating-II: Conduction Limit, *Combust. Flame* 28 (1977) 175–186.
- [16] I. Langmuir, The Evaporation of Small Spheres., *Phys. Rev. A* 12 (5) (1918) 368–370.
- [17] C. H. Wang, K. L. Pan, W. C. Huang, H. C. Wen, J. Y. Yang, and C. K. Law, Effects of fuel properties on the burning characteristics of collision-merged alkane/water droplets, *Exp. Therm. Fluid Sci.* 32 (5) (2008) 1049–1058
- [18] C. D. Rosebrock, T. Wriedt, and L. Mädler, The Role of Microexplosions in Flame Spray Synthesis for Homogeneous Nanopowders from Low-Cost Metal Precursors, *AIChE J.* 62 (2) (2016) 381–391.
- [19] K. Okai *et al.*, Pressure effects on combustion of methanol and methanol/dodecanol single droplets and droplet pairs in microgravity, *Combust. Flame* 121 (3) (2000) 501–512.
- [20] J. C. Chow *et al.*, The application of thermal methods for determining chemical composition of carbonaceous aerosols: A review, *J. Environ. Sci. Heal. - Part A Toxic/Hazardous Subst. Environ. Eng.*, 42 (11) (2007) 1521–1541.
- [21] D. Kittelson, Engines and nanoparticles: A review, *J. Aerosol Sci.* 29 (5) (1998) 575–588.